

# Entanglement fingerprint of a non-invertible symmetry: exact Fibonacci cut charges on the lattice

Yi Liang<sup>1,\*</sup>

<sup>1</sup>*Independent Researcher, Beijing, China*

(Dated: July 2, 2026)

Non-invertible defects are usually diagnosed through scaling spectra or infrared CFT data. We show that the Fibonacci duality defect of the critical golden chain already carries an exact categorical fingerprint at finite lattice size. The even-length antiferromagnetic ground state has fixed cut-charge weights, giving  $P_\tau/P_1 = \varphi^2$  and  $\ln g = \ln \varphi$  without finite-size extrapolation. The proof is a finite-dimensional operator identity for the sandwiched cut projectors, combined with a Perron–Frobenius sector theorem for the even-length ground state. This gives a sharp lattice-level boundary entropy for a non-Abelian duality defect. We also separate this exact two-charge result from the finer six-primary tricritical-Ising resolution: the latter is located by the standard scaling-limit Virasoro branching of  $A_4$  affine-TL packets, and is not an assumption in the finite-size theorem.

## INTRODUCTION

Non-invertible symmetries are categorical rather than group-like: fusion of their topological defect operators decomposes into sums of sectors instead of a single inverse element [1–6]. Their sharpest diagnostics are therefore not only spectra, but categorical data—quantum dimensions, defect fusion channels, and symmetry-resolved entanglement weights—that organize the Hilbert space. Existing diagnostics often proceed indirectly, through entanglement-spectrum statistics, finite-size CFT matching, or CFT and boundary-tube formulas for defect entropies [7–11]. Related periodic-MPS arc-gram transfer-matrix methods extract full contiguous-arc entanglement spectra in tensor-network settings [12]. Here we ask a more microscopic question: can a non-invertible defect leave an exact finite-size entanglement fingerprint, before any thermodynamic extrapolation is taken?

The Fibonacci golden chain is the minimal non-Abelian setting in which this question is nontrivial [13–15]. Its simple anyon  $\tau$  obeys  $\tau \otimes \tau = \mathbf{1} \oplus \tau$ , and the chain carries a non-invertible duality defect  $Y_\tau$  with the same Fibonacci fusion rule [16, 17]. At criticality the model flows to the tricritical Ising CFT  $\mathcal{M}(5, 4)$  with  $c = 7/10$ , where the defect admits a finer primary-channel description. The finite lattice, however, first sees the anyonic charge crossing a spatial cut,  $a \in \{\mathbf{1}, \tau\}$ . The relation between this exact cut-charge layer and the infrared primary-channel layer is the central issue.

We prove that, for the even-length antiferromagnetic periodic ground state, the cut-charge weights are fixed exactly:

$$P_a = \frac{d_a^2}{D^2}, \quad \frac{P_\tau}{P_1} = \varphi^2, \quad \ln g = \ln \varphi. \quad (1)$$

The result is not a fit to a leading Schmidt level or a large- $L$  extrapolation. It follows from a finite-dimensional sandwiched-projector identity for the  $Y_\tau = \varphi$  topological sector, plus a Perron–Frobenius proof that the

even- $L$  AFM ground state lies in that sector. The Fibonacci quantum dimensions are, of course, category data; the nontrivial point is that the interacting finite lattice ground state realizes their charge weights exactly, with no CFT tower fitting. In the Abelian Kramers–Wannier case the analogous program identifies the Ising quantum dimension from a Majorana entanglement zero mode [18]; here the same question is answered without a free-fermion solution.

This is a deliberately coarse but exact statement. The cut charge  $a \in \{\mathbf{1}, \tau\}$  is not the same as the six primary labels of the tricritical Ising CFT, and the Letter does not claim to construct six-primary lattice projectors. Instead it identifies the finite-lattice categorical layer that is already exact. The finer primary-channel layer is standard continuum data: in the  $A_4$  affine-TL description, the scaling-limit characters are organized by braid-translation packets whose Virasoro branching contains the six towers [19]. This separation is the point: the non-Abelian quantum dimension  $\varphi$  appears as an exact lattice charge ratio before the full infrared primary resolution is invoked.

## MODEL AND CUT-CHARGE SECTORS

The Fibonacci category has simple objects  $\mathbf{1}, \tau$  with  $d_{\mathbf{1}} = 1$ ,  $d_\tau = \varphi = (1 + \sqrt{5})/2$ , and  $D^2 = 1 + \varphi^2$ . We use the standard fusion-path representation of the golden chain, with Temperley–Lieb generators  $e_i$  normalized by

$$H = - \sum_i e_i = -\varphi \sum_i P_i, \quad e_i^2 = \varphi e_i, \quad e_i e_{i\pm 1} e_i = e_i, \quad (2)$$

where  $P_i = e_i/\varphi$  projects neighboring  $\tau$  anyons onto the vacuum channel [13]. The nontrivial associator is fixed by

$$F_\tau^{\tau\tau\tau} = \begin{pmatrix} \varphi^{-1} & \varphi^{-1/2} \\ \varphi^{-1/2} & -\varphi^{-1} \end{pmatrix}. \quad (3)$$

A periodic fusion path carries an anyonic charge across any spatial cut. Let  $\Pi_a^{(\ell)}$  denote the projector onto the cut charge  $a \in \{\mathbf{1}, \tau\}$  at bond  $\ell$ . The topological symmetry operator  $Y_\tau$  is obtained by inserting a  $\tau$  loop around the periodic chain. It obeys the Fibonacci fusion algebra

$$Y_\tau^2 = I + Y_\tau, \quad (4)$$

and therefore has eigenvalues  $\varphi$  and  $-1/\varphi$ . We write

$$E_+ = \frac{I + \varphi Y_\tau}{D^2} \quad (5)$$

for the orthogonal projector onto the  $Y_\tau = \varphi$  sector.

The theorem below concerns only this finite-lattice cut-charge resolution. It does not assume a decomposition into the six primary channels of the infrared  $\mathcal{M}(5,4)$  CFT. That finer resolution requires additional primary-channel projectors and is kept separate from the exact two-charge statement proved here.

## EXACT FINITE-SIZE CUT-CHARGE FINGERPRINT

### Cut-charge theorem

Let  $\Pi_a^{(\ell)}$  project onto the Fibonacci charge  $a \in \{\mathbf{1}, \tau\}$  crossing bond  $\ell$ , and let  $E_+$  be the projector in Eq. (5).

#### Theorem 1 (Finite-size cut-charge theorem)

For the critical periodic Fibonacci golden chain with Hamiltonian (2), the finite-lattice operator identity

$$E_+ \Pi_a^{(\ell)} E_+ = \frac{d_a^2}{D^2} E_+, \quad a \in \{\mathbf{1}, \tau\}, \quad (6)$$

holds for every cut  $\ell$ . For even  $L$ , the AFM ground state lies in this sector,  $E_+ \Omega_L = \Omega_L$ , and hence

$$P_a = \langle \Omega_L | \Pi_a^{(\ell)} | \Omega_L \rangle = \frac{d_a^2}{D^2},$$

$$P_\tau / P_{\mathbf{1}} = \varphi^2, \quad \ln g = \frac{1}{2} \ln(P_\tau / P_{\mathbf{1}}) = \ln \varphi. \quad (7)$$

The proof is finite dimensional. Put  $A = I + \varphi Y_\tau = D^2 E_+$  and decompose the periodic path space as  $\mathcal{H} = \mathcal{H}_{\mathbf{1}} \oplus \mathcal{H}_\tau$  according to the cut label. The local Fibonacci fusion rule gives the block  $(Y_\tau)_{\mathbf{1}\mathbf{1}} = 0$ , hence  $A_{\mathbf{1}\mathbf{1}} = I$ . Since  $E_+$  is an orthogonal projection, it remains to know its rank. A direct cyclic  $F$ -symbol trace gives  $\text{Tr} Y_\tau = (-1/\varphi)^L$ , while the fusion adjacency matrix  $N = \begin{pmatrix} 0 & 1 \\ 1 & 1 \end{pmatrix}$  gives  $\dim \mathcal{H}_{\mathbf{1}} = (N^L)_{\mathbf{1}\mathbf{1}}$ . Diagonalizing  $N$  yields  $\text{rank}(E_+) = (\text{Tr} N^L + \varphi(-1/\varphi)^L)/D^2 = (N^L)_{\mathbf{1}\mathbf{1}} = \dim \mathcal{H}_{\mathbf{1}}$ . Therefore  $\text{Ran}(E_+)$  is the graph of an isometry  $V : \mathcal{H}_{\mathbf{1}} \rightarrow \mathcal{H}_\tau$  and  $A = \begin{pmatrix} I & \varphi V^\dagger \\ \varphi V & \varphi^2 V V^\dagger \end{pmatrix}$ . This gives  $A \Pi_{\mathbf{1}}^{(\ell)} A = A$  and  $A \Pi_\tau^{(\ell)} A = \varphi^2 A$ , proving Eq. (6). Finally, Perron–Frobenius positivity of the even- $L$  AFM

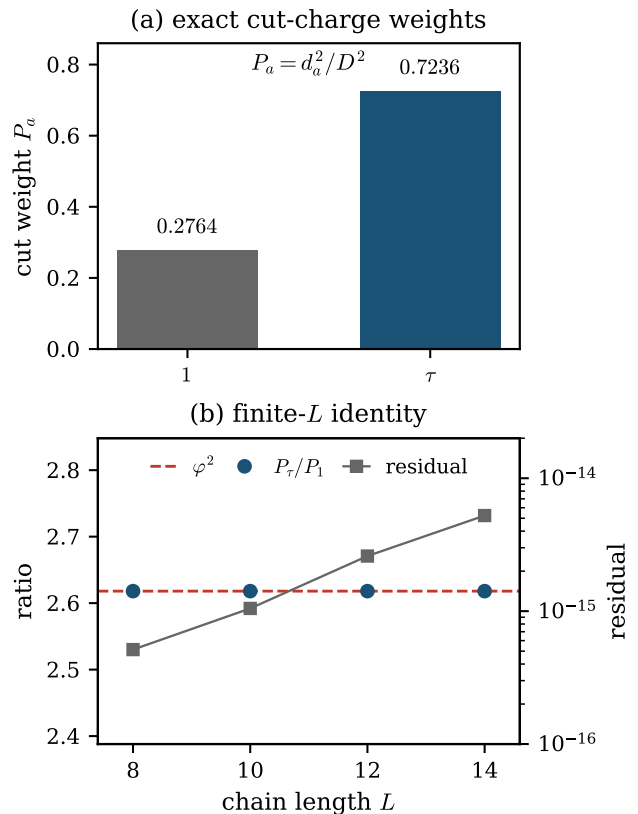


FIG. 1. Exact finite-size cut-charge fingerprint. (a) The two Fibonacci charge sectors carry fixed weights  $P_{\mathbf{1}} = 1/D^2 \approx 0.2764$  and  $P_\tau = \varphi^2/D^2 \approx 0.7236$ , obtained from the sandwiched-projector identity rather than from a large- $L$  extrapolation. (b) The ratio  $P_\tau/P_{\mathbf{1}}$  equals  $\varphi^2$  for every even  $L$ ; numerical verification on  $L = 8, 10, 12, 14$  confirms the identity to machine precision (residual  $< 5.3 \times 10^{-15}$ ).

Hamiltonian and the positivity of  $E_+ |\tau \cdots \tau\rangle$  place the unique ground state in the  $Y_\tau = \varphi$  sector.

Direct double-precision finite-matrix construction verifies the absolute operator residual

$$\|E_+ \Pi_a^{(\ell)} E_+ - (d_a^2/D^2) E_+\| < 5.3 \times 10^{-15} \quad (8)$$

for  $L = 8, 10, 12, 14$ . These checks audit the finite-dimensional proof; they are not used as an extrapolation. Thus the golden-ratio defect degeneracy is forced by the finite-lattice charge-resolution algebra, not by a thermodynamic fit.

### Physical consequence and resolution boundary

Equation (7) is the non-Abelian analogue of reading a duality-defect quantum dimension from entanglement. For the Fibonacci defect the answer is

$$\ln g = \ln \varphi = 0.481211825\dots, \quad (9)$$

obtained from an exact charge ratio rather than from fitting the leading Schmidt level. We use  $g$  as the defect degeneracy extracted operationally from the entanglement cut-charge ratio. The value matches the Affleck–Ludwig topological-defect degeneracy  $g = d_\tau$  [20, 21], but the derivation here is a finite-lattice charge-sector identity rather than a boundary partition function computation. The result is therefore a finite-size categorical fingerprint: a spatial cut sees the two Fibonacci charges with weights proportional to  $d_a^2$ .

This statement is intentionally not a six-primary projector claim. The infrared tricritical-Ising CFT has six primary channels, and modular data predict a finer Verlinde-polarization structure. The finite lattice theorem proved here resolves the exact Fibonacci cut charge  $\{\mathbf{1}, \tau\}$ . The primary-channel layer is a separate scaling-limit organization. In the standard  $A_4$  RSOS/affine-TL description, braid-translation packets have continuum Virasoro character branching

$$\mathrm{Tr}_{X_{0,q^{2n}}} q^{L_0-c/24} \bar{q}^{\bar{L}_0-c/24} = \sum_r \chi_{r,n}(q) \bar{\chi}_{r,n}(\bar{q}), \quad (10)$$

subject to the Kac reflection [19]. Thus the six-primary structure is not ignored, but neither this branching formula nor any finite-size source-algebra refinement is used in the proof of Eq. (6). The hierarchy is

$$\begin{aligned} \{\mathbf{1}, \tau\} \text{ cut charge} &\subsetneq \text{ affine-TL packets} \\ &\xrightarrow{L \rightarrow \infty} \text{ CFT primary towers.} \end{aligned} \quad (11)$$

As calibration, the same golden-chain data give  $c = 0.6998$  from the Casimir fit and defect gaps  $h + \bar{h} \simeq 3/40$  and  $3/5$  [21], consistent with the tricritical-Ising fixed point. These CFT checks identify the continuum theory; they are not inputs to the finite-size cut-charge proof. Conversely, the theorem identifies a categorical operator identity that acts before the continuum limit is taken.

## DISCUSSION

The result above turns the Fibonacci quantum dimension into a finite-size entanglement observable. The point

is not merely that the boundary entropy approaches  $\ln \varphi$  in the scaling limit, but that the even- $L$  interacting lattice ground state already realizes the categorical weights exactly:  $P_\tau/P_{\mathbf{1}} = \varphi^2$ . Compared with CFT, boundary-tube, or symmetry-resolved entanglement diagnostics of defect entropy [9–11, 22], the present result fixes a microscopic cut-charge ratio before the thermodynamic limit or full primary-channel resolution is invoked.

The proof also clarifies which part of the statement is category data and which part uses the Hamiltonian. The sandwiched identity follows from the local fusion rule  $(Y_\tau)_{\mathbf{1}\mathbf{1}} = 0$ , the cyclic  $F$ -symbol trace  $\mathrm{Tr}(Y_\tau) = (-1/\varphi)^L$ , and the resulting block-graph rank identity. The Hamiltonian enters only to select the physical sector: Perron–Frobenius positivity places the even- $L$  AFM ground state in  $E_+ \mathcal{H}$ . Thus the charge-resolution algebra is finite-dimensional category data, while the golden-chain interaction supplies the ground-state sector.

This is deliberately a two-charge theorem, not a finite-size six-primary projector construction. The lattice cut charge  $a \in \{\mathbf{1}, \tau\}$  is not a label for the six CFT primaries of  $\mathcal{M}(5, 4)$ . The latter enter through the standard scaling-limit branching of  $A_4$  affine-TL packets into Virasoro characters, Eq. (10); that branching is not an input to the finite-size proof. The theorem therefore locates the exact finite-lattice categorical layer while keeping the continuum primary-channel layer separate.

The same modular mechanism has higher-rank analogues. As a benchmark, the integer sector of  $\mathrm{su}(2)_5$  gives three Verlinde-polarization ratios fixed by the restricted modular  $S$  matrix; the numerical values are listed in the Supplemental Material. This is included only as a category-level target for future charge-resolution tests, not as a finite-lattice theorem for that model.

The finite-size theorem therefore provides a clean bridge between lattice anyon algebra and continuum defect physics: the non-Abelian quantum dimension is visible directly in Schmidt-sector weights, with cut charge resolved first and primary-channel refinement left to the scaling limit.

*Data and code availability.*—The code and data used to reproduce the finite-size checks and figure assets are available in a Zenodo software record [23].

## Supplemental Material

This Supplemental Material collects the technical details underlying the main text: the exact fusion-path superselection structure (Sec. S1), the complete proof of the finite-size cut-charge theorem for the even-length Fibonacci chain (Sec. S2), the rank-3  $\text{su}(2)_5$  modular-data benchmark (Sec. S3), and the direct finite-size numerical verification of the sandwiched-projector identity (Sec. S4). Equation and section numbers are prefixed by ‘‘S’’; references to unprefixed numbers refer to the main text.

### CUT-CHARGE THEOREM: COMPLETE PROOF

#### A. Fusion-path basis and exact superselection

The Hilbert space  $\mathcal{V}^{(\tau)}$  is the Fibonacci fusion-path space with a single  $\tau$ -insertion. Each basis state is an admissible height string  $|h_0, \dots, h_{L-1}\rangle$  in the  $A_4$  RSOS representation. A spatial bipartition cuts the chain at an internal bond  $\ell$ , which carries a definite anyon charge  $a_\ell \in \{\mathbf{1}, \tau\}$ . The reduced density matrix of the left half is exactly block diagonal in that charge,

$$\rho_A = \bigoplus_{a \in \{\mathbf{1}, \tau\}} \rho_A^{(a)}, \quad P_a \equiv \text{Tr} \rho_A^{(a)} = \sum_{k: c_k=a} \lambda_k^2, \quad (\text{S1})$$

where  $\{\lambda_k^2\}$  are Schmidt weights and  $c_k$  is the cut charge.

#### B. Two-charge theorem proof

Let  $\Omega_L$  be the nondegenerate AFM ground state for even  $L$ . The topological symmetry operator  $Y_\tau$  acts on the fusion-path basis by inserting a  $\tau$ -loop around the chain. Its possible eigenvalues are  $\varphi$  and  $-1/\varphi$ , as follows from the Fibonacci Verlinde formula  $S_{\tau a}/S_{\mathbf{1} a} = d_a$ . The point of Step 1 is to determine which of these two topological sectors contains the even- $L$  AFM ground state.

*Step 1: Ground-state eigenvalue.* The Hamiltonian  $H = -\varphi \sum_i P_i$  with  $P_i = e_i/\varphi$  is stoquastic: all off-diagonal matrix elements are non-positive in the fusion-path basis, because the local Temperley–Lieb projector  $P_i$  has matrix elements ( $A_4$  RSOS) only connecting admissible height configurations and carries a single-channel expansion in the Fibonacci planar algebra. The representation is irreducible for even  $L$ : the periodic fusion-path space  $\mathcal{V}^{(\tau)}$  is a single connected graph under the action of  $H$ , because the TL algebra generated by  $\{e_i\}$  at  $\delta = \varphi$  acts transitively on height configurations compatible with the single  $\tau$ -insertion [13, 14]. Perron–Frobenius therefore gives a unique ground state with strictly positive coefficients in the fusion-path basis. The topological symmetry  $Y_\tau$  commutes with  $H$ , so this state lies entirely in either the  $Y_\tau = \varphi$  sector or the  $Y_\tau = -1/\varphi$  sector.

To select the sector, let  $|T\rangle = |\tau\tau \dots \tau\rangle$  and consider  $u = E_+|T\rangle$ . We spell out the sign input. In the gauge used in the Letter, the nontrivial Fibonacci block has entries  $\varphi^{-1}, \varphi^{-1/2}, \varphi^{-1/2}, -\varphi^{-1}$ ; the only negative entry is the  $\tau\tau \rightarrow \tau\tau$  channel. In the cyclic hoop matrix element from the all- $\tau$  path to an output path  $y$ , all nonzero local factors are therefore positive except one factor  $-\varphi^{-1}$  for each adjacent  $\tau\tau$  pair in  $y$ . Hence

$$\text{sgn}\langle y|Y_\tau|T\rangle = (-1)^{N_{\tau\tau}(y)}, \quad (\text{S2})$$

where  $N_{\tau\tau}(y)$  is the number of adjacent  $\tau\tau$  pairs. Because admissible Fibonacci paths have no adjacent vacuum labels, each vacuum label removes two adjacent  $\tau\tau$  pairs from the all- $\tau$  cycle, so  $N_{\tau\tau}(y) = L - 2z(y)$  with  $z(y)$  the number of vacuum labels. Thus for even  $L$  every nonzero hoop contribution to  $E_+|T\rangle = (|T\rangle + \varphi Y_\tau|T\rangle)/D^2$  has positive sign, and the all- $\tau$  component is nonzero. Therefore  $u$  is a nonzero componentwise nonnegative vector. A positive Perron–Frobenius ground state has positive overlap with this vector; hence it cannot lie in the orthogonal  $E_-$  sector. Therefore

$$E_+\Omega_L = \Omega_L, \quad Y_\tau\Omega_L = \varphi\Omega_L. \quad (\text{S3})$$

For odd  $L$  the parity in the same sign calculation is reversed, so the above positivity witness no longer selects the  $E_+$  ground-state sector. Accordingly the finite-ground-state statement in the Letter is restricted to even  $L$ . We do not use, or claim, an automatic  $E_-$  replacement of Eq. (S18): replacing  $E_+$  by the complementary projector changes both

the relevant block normalization and the rank input, so it would require a separate finite-size sector analysis rather than a formal substitution.

*Step 2: Sandwiched projector identity.* This step is an operator identity on the periodic path space and does not use the ground state. Fix the cut and decompose

$$\mathcal{H}_L = \mathcal{H}_1 \oplus \mathcal{H}_\tau, \quad \mathcal{H}_a = \Pi_a^{(\ell)} \mathcal{H}_L. \quad (\text{S4})$$

Set

$$A = I + \varphi Y_\tau = D^2 E_+. \quad (\text{S5})$$

The local Fibonacci fusion rule gives the  $\mathbf{11}$  block  $(Y_\tau)_{\mathbf{11}} = 0$ : a single  $\tau$  hoop crossing a vacuum cut changes the cut channel to  $\tau$  and cannot return to vacuum. Hence

$$A_{\mathbf{11}} = I. \quad (\text{S6})$$

It remains to know the rank of  $E_+$ . Let  $N = \begin{pmatrix} 0 & 1 \\ 1 & 1 \end{pmatrix}$  be the Fibonacci fusion adjacency matrix. Then

$$\dim \mathcal{H}_L = \text{Tr}(N^L), \quad \dim \mathcal{H}_1 = (N^L)_{\mathbf{11}}. \quad (\text{S7})$$

The cyclic  $F$ -symbol formula for  $Y_\tau$  gives

$$\text{Tr}(Y_\tau) = (-1/\varphi)^L. \quad (\text{S8})$$

A direct verification: the matrix elements of  $Y_\tau$  in the fusion-path basis are

$$\langle y | Y_\tau | x \rangle = \prod_{i=0}^{L-1} F_{x_i y_{i+1}}^{\tau x_{i+1} y_i}, \quad x_L \equiv x_0, \quad y_L \equiv y_0, \quad (\text{S9})$$

where  $F$  is the Fibonacci  $F$ -symbol used in the main text and indices run over  $\{\mathbf{1}, \tau\}$ . For the diagonal  $y = x$ , the local factor  $F_{x_i x_{i+1}}^{\tau x_{i+1} x_i}$  vanishes unless  $x_i = x_{i+1} = \tau$ : a  $\mathbf{1} \rightarrow \tau \rightarrow \mathbf{1}$  or  $\mathbf{1} \rightarrow \mathbf{1} \rightarrow \mathbf{1}$  local loop has zero amplitude in the Fibonacci  $F$ -symbol. The only surviving diagonal path is the all- $\tau$  configuration  $x = (\tau, \tau, \dots, \tau)$ , for which each local factor equals  $F_{\tau\tau\tau}^{\tau\tau\tau} = -1/\varphi$ . Multiplying  $L$  identical factors gives Eq. (S8). Since  $E_+$  is an orthogonal projection,

$$\text{rank}(E_+) = \text{Tr}(E_+) = \frac{\text{Tr}(N^L) + \varphi(-1/\varphi)^L}{D^2} = (N^L)_{\mathbf{11}} = \dim \mathcal{H}_1, \quad (\text{S10})$$

where the penultimate equality follows by diagonalizing  $N$ , whose eigenvalues are  $\varphi$  and  $-1/\varphi$ . This rank computation uses only the cyclic trace of  $Y_\tau$  and the Fibonacci path-counting matrix; it is independent of the sandwiched-projector identity that follows.

Now we extract the block structure of  $A$  from the two inputs Eqs. (S6) and (S10).

*Lemma (Projection graph lemma).* Let  $P$  be an orthogonal projection on  $\mathcal{H}_1 \oplus \mathcal{H}_\tau$  and set  $A = D^2 P$  with  $D^2 = 1 + \varphi^2$ . If

$$A_{\mathbf{11}} = I_{\mathcal{H}_1}, \quad \text{rank}(A) = \dim \mathcal{H}_1, \quad (\text{S11})$$

then  $\text{Ran}(P)$  is the graph of a linear map  $T : \mathcal{H}_1 \rightarrow \mathcal{H}_\tau$  satisfying  $T^\dagger T = \varphi^2 I$ , i.e.  $T = \varphi V$  with  $V$  an isometry. Equivalently

$$A = \begin{pmatrix} I & \varphi V^\dagger \\ \varphi V & \varphi^2 V V^\dagger \end{pmatrix}. \quad (\text{S12})$$

*Proof of the lemma.* Let  $S = \text{Ran}(P)$  and let  $\pi_1$  denote orthogonal projection from  $\mathcal{H}_1 \oplus \mathcal{H}_\tau$  onto  $\mathcal{H}_1$ . The hypothesis gives  $\dim S = \text{rank}(P) = \text{rank}(A) = \dim \mathcal{H}_1$  and

$$P_{\mathbf{11}} = \pi_1 P \pi_1^\dagger = \frac{1}{D^2} I_{\mathcal{H}_1}. \quad (\text{S13})$$

Equivalently, for the map  $Q : S \rightarrow \mathcal{H}_1$  obtained by restricting  $\pi_1$  to  $S$ , one has  $Q Q^\dagger = I/D^2$ . Thus  $Q$  is surjective; since its domain and codomain have the same finite dimension,  $Q$  is bijective. Hence every  $x \in \mathcal{H}_1$  has a unique lift in  $S$ , so  $S$  is the graph of a unique linear map  $T : \mathcal{H}_1 \rightarrow \mathcal{H}_\tau$ :

$$\text{Ran}(P) = \{(x, Tx) : x \in \mathcal{H}_1\}. \quad (\text{S14})$$

The orthogonal projector onto a graph has the standard block form

$$P_{\text{graph}} = \begin{pmatrix} (I + T^\dagger T)^{-1} & (I + T^\dagger T)^{-1} T^\dagger \\ T(I + T^\dagger T)^{-1} & T(I + T^\dagger T)^{-1} T^\dagger \end{pmatrix}. \quad (\text{S15})$$

Equating  $P_{11} = I/D^2$  with the top-left block of Eq. (S15) gives  $(I + T^\dagger T)^{-1} = I/D^2$ , hence  $T^\dagger T = (D^2 - 1)I = \varphi^2 I$ . Therefore  $T = \varphi V$  with  $V^\dagger V = I$ . Substituting into Eq. (S15) and multiplying by  $D^2$  yields Eq. (S12).  $\square$

*Compact algebraic alternative.* The block form can also be read directly from  $A^2 = D^2 A$ , which follows from  $A = I + \varphi Y_\tau$ ,  $Y_\tau^2 = I + Y_\tau$ , and  $\varphi^2 = \varphi + 1$ :

$$A^2 = I + 2\varphi Y_\tau + \varphi^2 Y_\tau^2 = I + 2\varphi Y_\tau + \varphi^2(I + Y_\tau) = D^2(I + \varphi Y_\tau) = D^2 A. \quad (\text{S16})$$

Write  $A$  in block form  $A = \begin{pmatrix} I & B^\dagger \\ B & C \end{pmatrix}$ , where  $B: \mathcal{H}_1 \rightarrow \mathcal{H}_\tau$ , with  $A_{11} = I$  from Eq. (S6). The  $(1, 1)$  block of  $A^2 = D^2 A$  gives  $I + B^\dagger B = D^2 I$ , hence  $B^\dagger B = \varphi^2 I$ . By singular-value decomposition  $B = \varphi V$  with  $V^\dagger V = I$ . Since  $A \geq 0$  and  $A_{11} = I$  has full rank, the Schur complement of  $A$  vanishes:  $C = B B^\dagger$ . Thus  $C = (\varphi V)(\varphi V^\dagger) = \varphi^2 V V^\dagger$ , recovering Eq. (S12). This algebraic path is independent of the graph-projection lemma; the two derivations cross-check each other.

Applying this lemma with  $P = E_+$  and  $A = D^2 E_+$ , the block form Eq. (S12) follows directly from Eqs. (S6) and (S10). Therefore

$$A \Pi_1^{(\ell)} A = A, \quad A \Pi_\tau^{(\ell)} A = A^2 - A = (D^2 - 1)A = \varphi^2 A. \quad (\text{S17})$$

Dividing by  $D^4$  proves

$$E_+ \Pi_1^{(\ell)} E_+ = \frac{1}{D^2} E_+, \quad E_+ \Pi_\tau^{(\ell)} E_+ = \frac{\varphi^2}{D^2} E_+. \quad (\text{S18})$$

This is the advertised sandwiched identity. Equivalently, the block form above says that the overlap between the vacuum-tube subspace  $E_+ \mathcal{H}_L$  and the cut-charge subspace  $\mathcal{H}_1$  is a scalar isometry: all nonzero singular values of  $E_+ \Pi_1^{(\ell)}$  are exactly  $1/D$ . Thus the tube-flux and cut-charge resolutions are crossed bases inside the vacuum sector. Notice that no commutation of  $\Pi_a^{(\ell)}$  with  $H$  or  $Y_\tau$  is assumed; in fact the unsandwiched and commutator versions are false.

*Step 3: Sector weights and  $g$ -function.* Taking the expectation in the even- $L$  ground state and using Eq. (S3),

$$\begin{aligned} P_a &= \langle \Omega_L | \Pi_a^{(\ell)} | \Omega_L \rangle = \langle \Omega_L | E_+ \Pi_a^{(\ell)} E_+ | \Omega_L \rangle \\ &= \frac{d_a^2}{D^2} \langle \Omega_L | E_+ | \Omega_L \rangle = \frac{d_a^2}{D^2}. \end{aligned} \quad (\text{S19})$$

Hence  $P_\tau/P_1 = \varphi^2$  and  $\ln g = \frac{1}{2} \ln(P_\tau/P_1) = \ln \varphi$ .

### C. Rank-3 numerical benchmark: $\text{su}(2)_5$ integer sector

The finite-size proof above uses only Fibonacci fusion data plus the Hamiltonian input that the ground state lies in the  $Y_\tau = \varphi$  sector. A useful higher-rank benchmark is the integer sector  $a \in \{0, 1, 2\}$  of  $\text{su}(2)_5$ . Its normalized restricted modular matrix is

$$S_{ab} = \sqrt{\frac{4}{7}} \sin \frac{\pi(2a+1)(2b+1)}{7}. \quad (\text{S20})$$

For the  $a = 1$  Verlinde defect, the sector eigenvalues are  $\lambda_b = S_{1b}/S_{0b}$ . Thus the predicted polarization ratios are

$$r_b = |\lambda_b|^2: \quad r_0 = d_1^2, \quad r_1 = \left(\frac{d_2}{d_1}\right)^2, \quad r_2 = \frac{1}{d_2^2}, \quad (\text{S21})$$

where  $d_1 = \sin(3\pi/7)/\sin(\pi/7) = 2.24698\dots$  and  $d_2 = \sin(5\pi/7)/\sin(\pi/7) = 1.80194\dots$ . Numerically,

$$(r_0, r_1, r_2) = (5.0489\dots, 0.6431\dots, 0.3080\dots). \quad (\text{S22})$$

The same ratios are implemented in the numerical benchmark script `su2.5_verlinde_ratios.jl`, which checks the normalized restricted  $S$  matrix and prints the three Verlinde polarization ratios. This rank-3 pattern is not a Fibonacci identity in disguise: it has three distinct polarization values fixed by the modular  $S$  matrix. The benchmark is included as category-level support and a numerical target audit; the Letter proves the exact finite-lattice sandwiched-projector theorem for the Fibonacci chain.

## D. Numerical verification

A Julia script constructs the finite periodic Fibonacci path basis and the matrix representation of  $Y_\tau$  for  $L = 8, 10, 12, 14$ , then evaluates the finite-dimensional operator identities for  $E_+ \Pi_\alpha^{(\ell)} E_+$  directly. All residuals are  $< 10^{-14}$ . Code: `verify_sandwiched_projector_identity_2026.06.24.jl` in the reproducibility package.

## REFERENCES

- 
- \* [iantrans2042@gmail.com](mailto:iantrans2042@gmail.com)
- [1] D. Gaiotto, A. Kapustin, N. Seiberg, and B. Willett, Generalized global symmetries, *J. High Energy Phys.* **02** (02), 172, [arXiv:1412.5148](https://arxiv.org/abs/1412.5148).
  - [2] L. Bhardwaj and Y. Tachikawa, On finite symmetries and their gauging in two dimensions, *J. High Energy Phys.* **03** (03), 189, [arXiv:1704.02330](https://arxiv.org/abs/1704.02330).
  - [3] J. McGreevy, Generalized symmetries in condensed matter, *Annu. Rev. Condens. Matter Phys.* **14**, 57 (2023), [arXiv:2204.03045](https://arxiv.org/abs/2204.03045).
  - [4] F. Apruzzi, F. Bonetti, I. García Etxebarria, S. S. Hosseini, and S. Schäfer-Nameki, Symmetry TFTs from string theory, *Commun. Math. Phys.* **402**, 895 (2023), [arXiv:2112.02092](https://arxiv.org/abs/2112.02092).
  - [5] J. Kaidi, K. Ohmori, and Y. Zheng, Kramers–wannier-like duality defects in (3+1)d gauge theories, *Phys. Rev. Lett.* **128**, 111601 (2022), [arXiv:2111.01141](https://arxiv.org/abs/2111.01141).
  - [6] J. Kaidi, K. Ohmori, and Y. Zheng, Symmetry TFTs for non-invertible defects, *Commun. Math. Phys.* **404**, 1021 (2023), [arXiv:2209.11062](https://arxiv.org/abs/2209.11062) [[hep-th](#)].
  - [7] H. Li and F. D. M. Haldane, Entanglement spectrum as a generalization of entanglement entropy: Identification of topological order in non-abelian fractional quantum hall effect states, *Phys. Rev. Lett.* **101**, 010504 (2008), [arXiv:0805.0332](https://arxiv.org/abs/0805.0332) [[cond-mat.mes-hall](#)].
  - [8] P. Calabrese and A. Lefevre, Entanglement spectrum in one-dimensional systems, *Phys. Rev. A* **78**, 032329 (2008), [arXiv:0806.3059](https://arxiv.org/abs/0806.3059).
  - [9] Y. Choi, B. C. Raychaudhuri, and Y. Zheng, Noninvertible symmetry-resolved affleck-ludwig-cardy formula and entanglement entropy from the boundary tube algebra, *Phys. Rev. Lett.* **133**, 251602 (2024), [arXiv:2409.02806](https://arxiv.org/abs/2409.02806).
  - [10] P. Saura-Bastida, A. Das, G. Sierra, and J. Molina-Vilaplana, Categorical-symmetry resolved entanglement in conformal field theory, *Phys. Rev. D* **109**, 105026 (2024), [arXiv:2402.06322](https://arxiv.org/abs/2402.06322).
  - [11] A. Das, J. Molina-Vilaplana, and P. Saura-Bastida, Generalized symmetry resolution of entanglement in conformal field theory for twisted and anyonic sectors, *Phys. Rev. D* **110**, 125005 (2024), [arXiv:2409.02162](https://arxiv.org/abs/2409.02162).
  - [12] Y. Liang and C. Qian, True periodic boundary conditions in DMRG: Arc-Gram transfer-matrix method for entanglement entropy (2026), submitted to *SciPost Physics*.
  - [13] A. Feiguin, S. Trebst, A. W. W. Ludwig, M. Troyer, A. Kitaev, Z. Wang, and M. H. Freedman, Interacting anyons in topological quantum liquids: The golden chain, *Phys. Rev. Lett.* **98**, 160409 (2007), [arXiv:cond-mat/0612341](https://arxiv.org/abs/cond-mat/0612341).
  - [14] C. Gils, E. Ardonne, S. Trebst, D. A. Huse, A. W. W. Ludwig, M. Troyer, and Z. Wang, Anyonic quantum spin chains: Spin-1 generalizations and topological stability, *Phys. Rev. B* **87**, 235120 (2013), [arXiv:1303.4290](https://arxiv.org/abs/1303.4290).
  - [15] A. Kitaev, Anyons in an exactly solved model and beyond, *Ann. Phys.* **321**, 2 (2006), [arXiv:cond-mat/0506438](https://arxiv.org/abs/cond-mat/0506438).
  - [16] J. Belletête, A. M. Gainutdinov, J. L. Jacobsen, H. Saleur, and T. S. Tavares, Topological defects in periodic rsos models and anyonic chains (2020), [arXiv:2003.11293](https://arxiv.org/abs/2003.11293) [[math-ph](#)].
  - [17] D. Aasen, P. Fendley, and R. S. K. Mong, Topological defects on the lattice: Dualities and degeneracies (2020), [arXiv:2008.08598](https://arxiv.org/abs/2008.08598) [[cond-mat.stat-mech](#)].
  - [18] Y. Liang, Entanglement-spectrum fingerprint of a non-invertible symmetry: the Kramers–Wannier duality defect on the lattice (2026), submitted concurrently.
  - [19] J. Belletête, A. M. Gainutdinov, J. L. Jacobsen, H. Saleur, and R. Vasseur, On the correspondence between boundary and bulk lattice models and (logarithmic) conformal field theories, *J. Phys. A: Math. Theor.* **50**, 484002 (2017), [arXiv:1705.07769](https://arxiv.org/abs/1705.07769).
  - [20] I. Affleck and A. W. W. Ludwig, Universal noninteger "ground-state degeneracy" in critical quantum systems, *Phys. Rev. Lett.* **67**, 161 (1991).
  - [21] I. Makabe and G. M. T. Watts, Defects in the tri-critical ising model, *J. High Energy Phys.* (09), 013, [arXiv:1703.09148](https://arxiv.org/abs/1703.09148).
  - [22] J. Heymann and T. Quella, Revisiting the symmetry-resolved entanglement for noninvertible symmetries in 1+1d conformal field theories, *Phys. Rev. D* **112**, 025004 (2025), [arXiv:2409.02315](https://arxiv.org/abs/2409.02315).
  - [23] Y. Liang, Code for: Entanglement fingerprint of a non-invertible symmetry: exact Fibonacci cut charges on the lattice (2026).